

# A SAW resonator with two-dimensional reflectors

Marc Solal, Julien Gratier and Taeho Kook

TriQuint Semiconductor Inc.

Apopka, Florida, USA

Corresponding email: marc.solal@tqs.com

**Abstract**— It is known that a part of the loss of Leaky SAW resonators is due to radiation of acoustic energy in the bussbars. A lot of researchers are working on so called “Phononic crystals”. A 2D grating of very strong reflectors allows these devices to fully reflect, for a given frequency band, any incoming wave. A new device, based on the superposition of a regular SAW resonator and of a 2D periodic grating of reflectors, is proposed. Several arrangements and geometries of the reflectors were studied and compared experimentally on 48 degrees rotated Y cut Lithium Tantalate. In particular, a very narrow aperture ( $7.5 \lambda$ ) resonator was manufactured on 48 deg. LT in the 900 MHz range. Due to its small size, this resonator has a resonance Q of only 575 when using the standard technology while a resonance Q of 1100 was obtained for the new device without degradation of the other characteristics. Due to the narrow aperture, the admittance of the standard resonator showed a very strong parasitic above the resonance frequency while this effect is drastically reduced for the new device. These results demonstrate the feasibility of the new approach.

## I. INTRODUCTION

In SAW resonators, the energy is confined by placing a transducer between two reflectors. If this is a relatively efficient confinement, it is only working for the waves propagating perpendicularly to the electrodes. In the case of Leaky SAW on Lithium tantalate, it is now well known that some energy is leaking of the resonator in the other directions. In particular, due to the configuration of the slowness curves inside the resonator and in the bussbars, Leaky SAW radiation occurs in the bussbars. This so called “banana” effect produces losses above the resonance frequencies [1]. It was also shown that Rayleigh waves are leaking causing also some increase of loss [2]. Thus, one can expect improving the confinement of the waves in the transverse direction would lead to lower loss SAW devices.

In the mean time, researchers are working very actively on “phononic crystals”. The main goal here is to find structures presenting a band gap, i.e. able to fully reflect acoustic waves coming from any direction in a given frequency band, called

band gap. Usually, these phononic crystal are constituted of very strong reflectors like deep holes placed inside a bidimensional periodic grating. The possibility of obtaining a band gap for SAW [3] was demonstrated. But, the authors of this paper are not aware of any practical application for these devices.

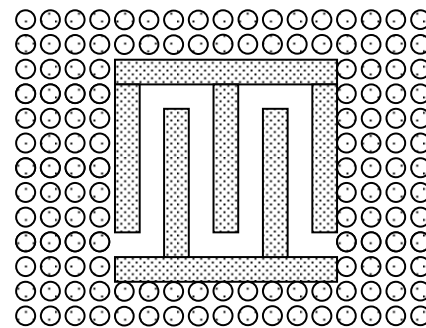


Figure 1. SAW resonator using an IDT inside a phononic crystal. This resonator is expected to have a lot of spurious modes

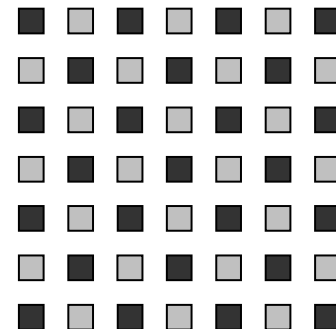


Figure 2. Hypothetical 2D IDT made by a grating of metallic reflectors at the surface of a piezoelectric substrate. The clear reflectors have to be connected to one electrical potential while the dark ones have to be connected to the other electrical potential.

The starting point of this work was to try to using the very nice properties of phononic crystals to reduce the losses of SAW resonators. The first natural idea (figure 1) is to place an

interdigitated transducer (IDT) inside a phononic crystal. In this case, assuming that the crystal is perfect, no energy can leak from the transducer, for any direction in the surface plane. Even if the technological challenges associated with this approach are solved, the main problem foreseen is the probable existence of several unwanted modes due to the large length and width of the transducer. The second natural idea, would be (figure 2), similarly to the IDT, to use metallic structures as reflectors and to connect them to different electrical potentials. A priori, this is a very attractive idea and less spurious modes can be expected as well as good Qs. Unfortunately, the interconnection for this structure makes its realization difficult.

The device described here is intermediary between this 2D IDT and a regular resonator. In order to avoid spurious modes, the 2D reflectors have to cover all the surface of the device. Traditional IDTs are a very convenient way to excite acoustic waves. The resonator shown in figure 3 is a superposition of a standard SAW resonator with a two-dimensional grating of reflectors. This new device uses the IDT for generating the acoustic energy while the 2D grating should prevent the leaking of acoustic energy in all directions.

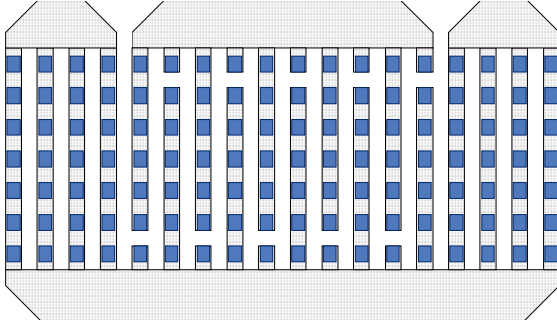


Figure 3. Principle of the new resonator. A standard SAW resonator (in grey) is superposed to a 2D periodic grating of reflectors.

## II. DESIGN CONSIDERATIONS

The main goal of this study was to reduce the losses for LSAW resonators on Lithium Tantalate. Aluminum was chosen as the material for the transducer. Because of its strong acoustic contrast with aluminum as well as for processing reasons, tungsten was chosen as material for the reflectors of the 2D grating. The  $Y+48^\circ$  orientation was chosen for the piezoelectric substrate.

### A. Simulation of the metal thickness influence

It is impossible to rigorously simulate the resonator of figure 3 using standard 2D SAW models. Thus, it was decided to approximate the dots by a uniform metallic layer above the aluminum. A finite transducer FEM/BEM software similar to the one described for example in [4] was used. This simulation could not predict the radiation or non radiation of acoustic energy outside of the resonator. The goal was rather to choose wisely the thicknesses of aluminum and tungsten in order to prevent bulk radiation losses.

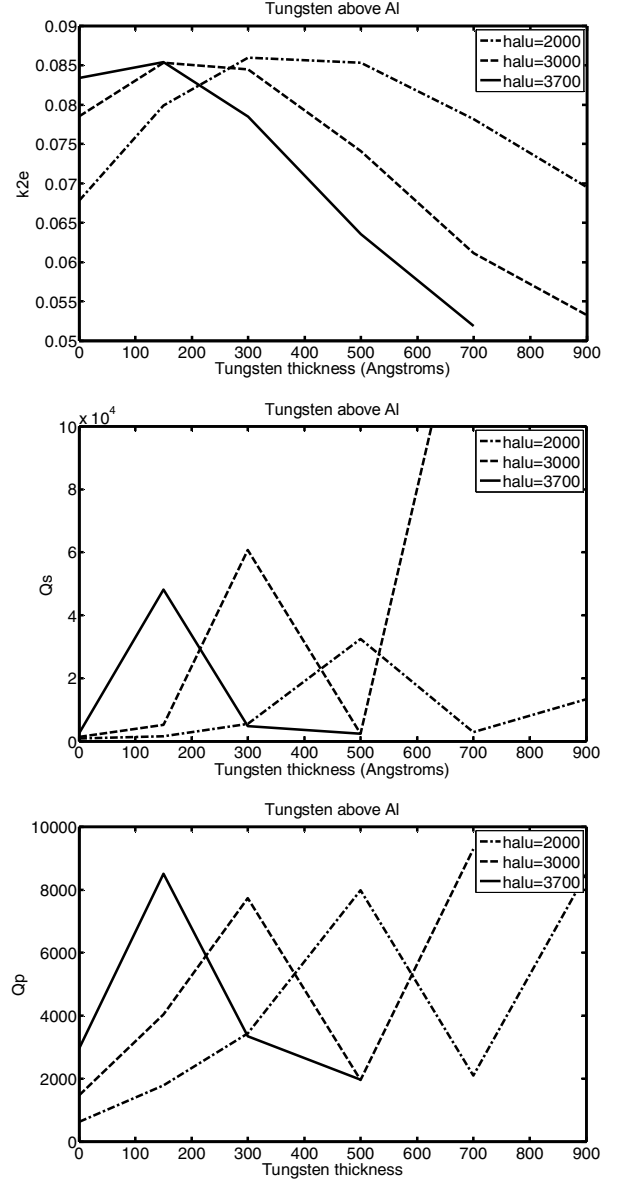


Figure 4. Simulation results for a resonator using tungsten above aluminum. The metallic films are assumed uniform in the transverse direction. Top coupling coefficient  $k_{2e}$ , center quality factor  $Q_s$  at serie resonance, bottom quality factor at parallel resonance (antiresonance)  $Q_p$

The chosen resonator for the simulation comprised 200 electrodes in the transducer and 50 in each grating. The period was  $2\mu m$ . Figure 4 shows the simulated variation with the tungsten thickness of the quality factor  $Q_s$  at resonance, the quality factor at antiresonance  $Q_p$  and the equivalent coupling factor defined as:

$$k_e^2 = \frac{\pi f_s}{2 f_p} \cdot \frac{1}{\tan \frac{\pi f_s}{2 f_p}}$$

where  $f_s$  and  $f_p$  are respectively the resonance and antiresonance frequencies. Various aluminum thicknesses

were simulated.. Both the resistive losses and the mechanical losses in the electrodes were neglected in these simulations. According to the results shown on fig. 4, the optimum tungsten thickness is depends on the aluminum thickness. For an aluminum thickness of 3700 Å, the maximum tungsten thickness to choose is about 150 angstroms. This would correspond to 300 angstroms assuming tungsten dots covering half of the surface of the transducers

### B. Definition of the test devices

To test the validity of this approach a mask with a set of test devices was defined. The resonator described previously (50 electrodes grating, 200 electrodes transducer, period between successive electrodes 2 µm, horizontal duty factor 50%) was chosen. Two different configurations for the dots were examined: the one of fig. 3 where the successive dot are aligned and the “staggered” one shown on figure 6 where the dots are shifted by half the vertical period between two successive electrodes.

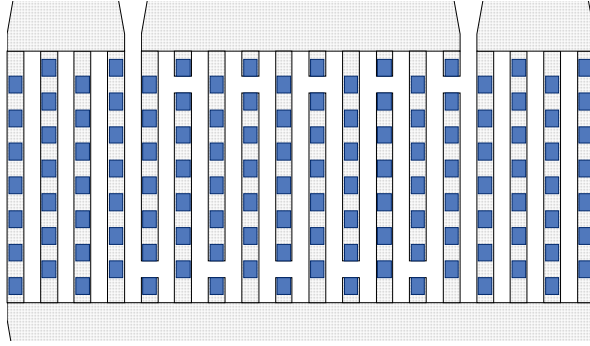


Figure 5. “Staggered” version of the resonator. The dots on two successive electrodes are shifted by half the vertical period.

As shown on figures 3 and 5, the acoustic aperture of the transducer has to be proportional to the vertical period in order to avoid one dot-reflector to short circuit the transducer. The vertical period was chosen similar to the horizontal period. To demonstrate the suppression of the transverse leakage, one of the apertures was chosen to be 15 vertical periods which is very narrow. The different variants are shown on table 1. The vertical period, the vertical duty factor-i.e. the ratio height of the dots to the vertical period- as well as the aperture were varied on the mask.

Configurations	Staggered	Aligned			
Aperture in vertical periods	15	30			
Vertical duty factor	0.4	0.5	0.6		
Vertical period ( $\mu\text{m}$ )	1.8	1.9	2.0	2.1	2.2

TABLE I. LIST OF THE VARIANTS ON THE MASK

## III. EXPERIMENTAL RESULTS

### A. Manufacturing process

A standard dry etch process was used for both the aluminum and the tungsten layer. The critical issues addressed when defining the process were: avoiding a misalignment of the mask levels and avoiding etching of the substrate when etching the tungsten. This was made easier by using the different nature of the films and the good selectivity of their etchers. The metal thicknesses were 3700 Å for the aluminum and 300 and 500 Å for the tungsten.

### B. Results for the devices without dots (reference)

As a reference, some wafers were processed using the standard aluminum metal film without adding the dots. Figure 6 shows the impedance curves as well as the smith charts for these resonators. It is seen clearly on these curves that a lot of loss happens above the resonance frequency. This effect is especially true for the narrow aperture resonator and the response is very similar to the “banana effect”. As expected, very narrow aperture resonators have a lot of losses.

### C. Results for the devices with the dots

It was found that the results were in general better for the 300 Å tungsten devices. This is shown on figure 7 for one particular configuration (aligned configuration, aperture 15 vertical periods, vertical period 2 µm, vertical duty factor 0.6). The 500 Å tungsten thickness had a degraded Q at antiresonance, probably due to the too large electrode mass.

Figure 8-9 show the responses obtained respectively for the staggered and aligned dots configurations. Figure 10-11 show the extracted coupling and quality factors for the different configurations of dots. The dots allow to improve all characteristics of the narrow aperture resonators. Surprisingly, this result is relatively insensitive to the dot configuration, vertical period and vertical duty factor. For example for the narrow aperture staggered configuration resonator with a vertical period of 2.2 µm and a vertical duty factor of 0.6, the quality factor at resonance was improved by a factor 2 while the quality factor at antiresonance was improved from about 600 to about 750. The coupling coefficient was also slightly improved.

## IV. CONCLUSION

A new resonator structure using the superposition of a standard resonator and of 2D grating of reflectors similar to phononic crystals was investigated. Even if the new device is difficult to model, experimental electrical results show that the new approach allows to suppress successfully the spuri above the resonance frequency for narrow aperture resonators. This suppresses the need to make a trade off between resistive losses (for wide apertures) and acoustic leakage losses (for narrow apertures). For narrow apertures, an increase of about a factor 2 of the quality factor at resonance was obtained while the other parameters are also improved.

It is not entirely certain today that the new device is really working how it was anticipated. It is also not clear if the individual reflectivity is large enough to obtain a true band gap. Despite all these unknowns, the new device fulfills its original requirements. More investigations are on the way to understand better the operation of the device and improve its performance.

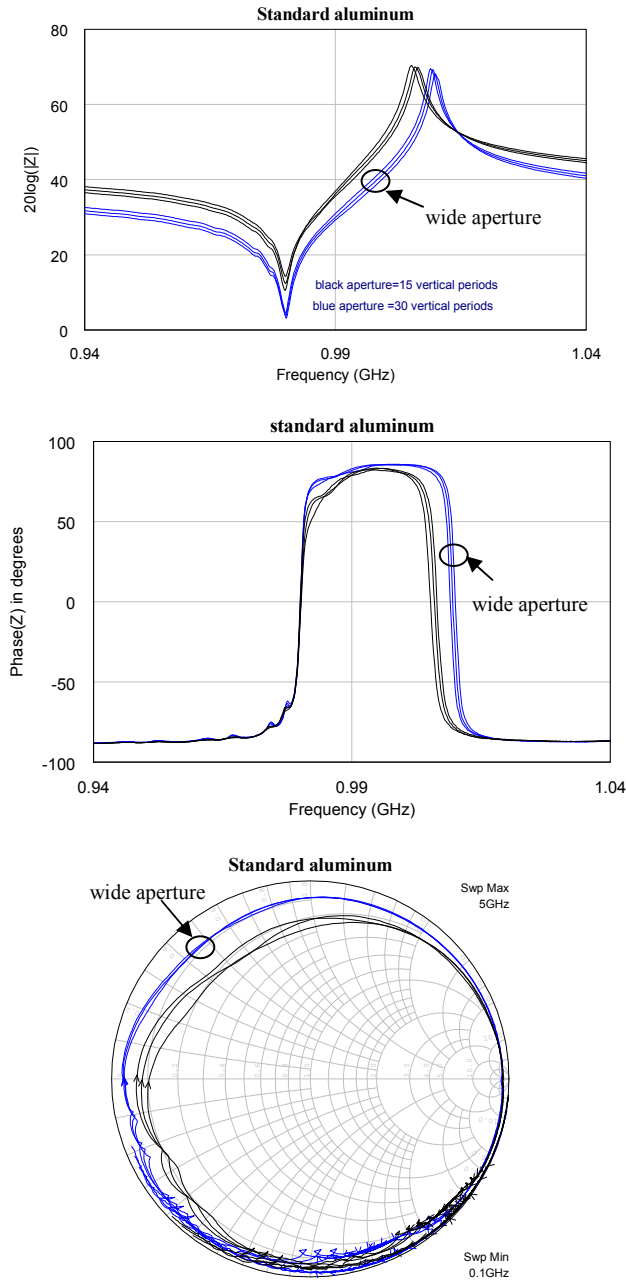


Figure 6. Comparison measurements of the wide aperture (dashed line, blue) and narrow aperture (full line, black) resonators when only aluminum is used. Top: impedance module, center: impedance phase, bottom: Smith chart.

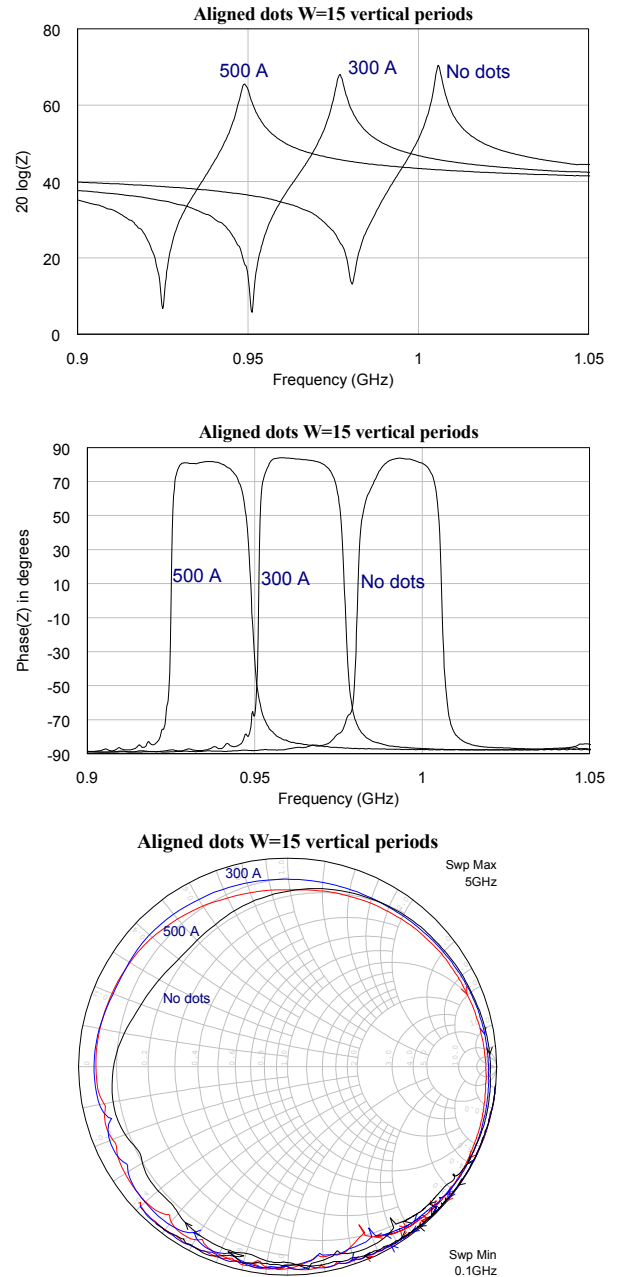


Figure 7. Effect of the tungsten thickness on the measured responses for the aligned dots narrow aperture resonators. The vertical period is 2  $\mu\text{m}$  and the vertical duty factor = 0.6. Top: impedance amplitude, center impedance phase, bottom Smith chart.

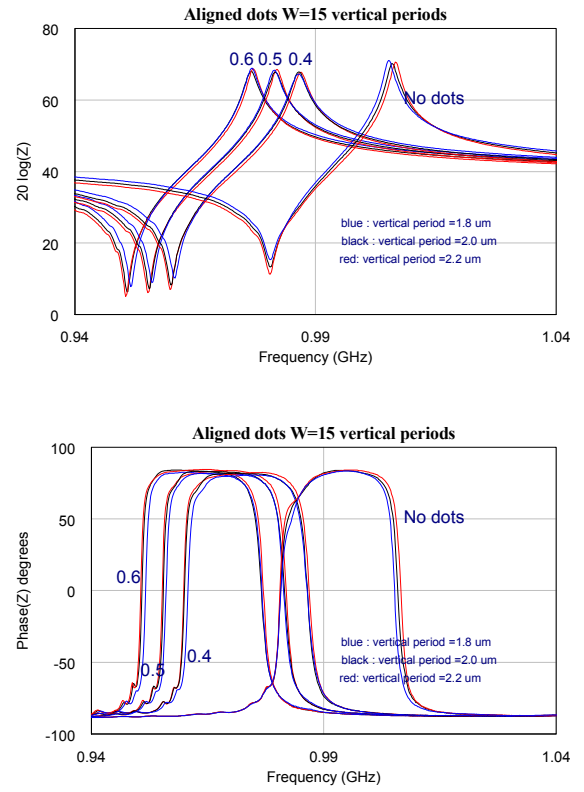
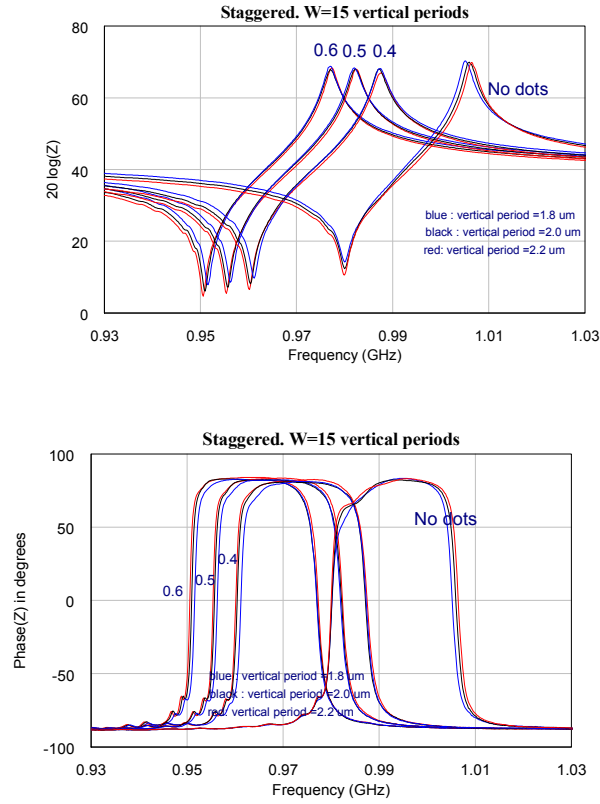


Figure 8. Results obtained for the narrow aperture resonators and the staggered arrangement. Top: Impedance module, middle impedance phase, bottom smith chart. For the two impedance curves, the higher frequency responses correspond to the devices without tungsten while the different groups of responses correspond to the different vertical duty factors. The blue, black and red curve correspond respectively to vertical periods of 1.8  $\mu\text{m}$ , 2  $\mu\text{m}$  and 2.2  $\mu\text{m}$ . On the Smith chart, the black curves correspond to the device without tungsten and the blue curve correspond to the devices with tungsten

Figure 9. Results obtained for the narrow aperture resonators and the staggered arrangement. Top: Impedance module, middle impedance phase, bottom Smith chart. For the two impedance curves, the higher frequency responses correspond to the devices without tungsten while the different groups of responses correspond to the different vertical duty factors. The blue, black and red curve correspond respectively to vertical periods of 1.8  $\mu\text{m}$ , 2  $\mu\text{m}$  and 2.2  $\mu\text{m}$ . On the Smith chart, the black curves correspond to the device without tungsten and the blue curve correspond to the devices with tungsten

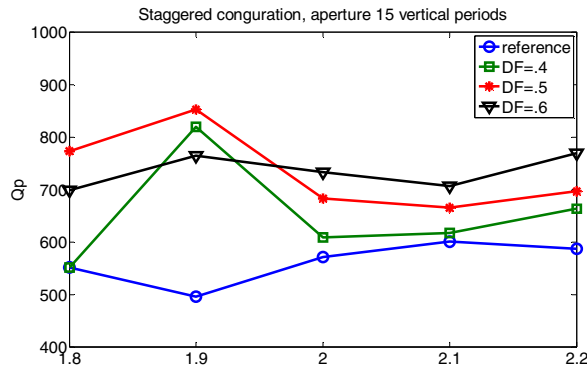
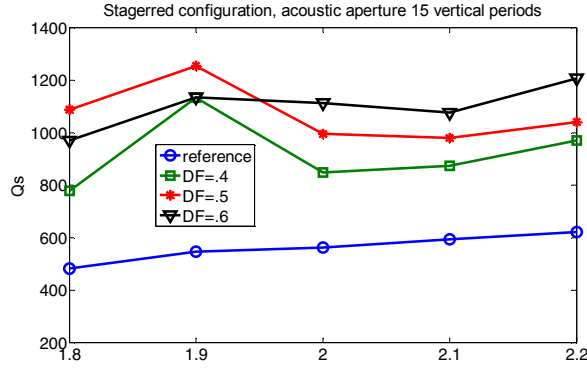
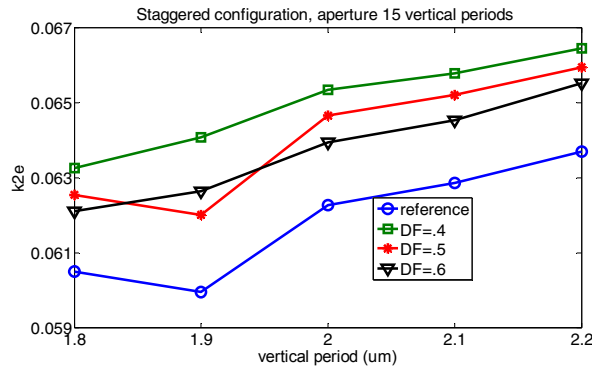


Figure 10. Experimental results for for the staggered dots devices in function of the vertical period in  $\mu\text{m}$ . The different curves correspond to the different vertical duty factors. The blue/circle symbols curve corresponds to the devices without tungsten dots. Top :coupling coefficient,Center: quality factor at resonance  $Q_s$  Bottom: quality factor at antiresonance  $Q_p$  (bottom)

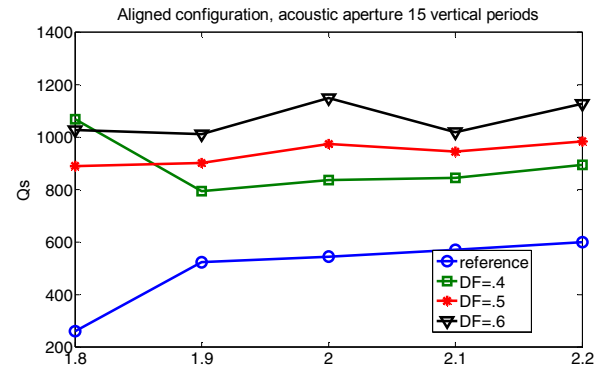
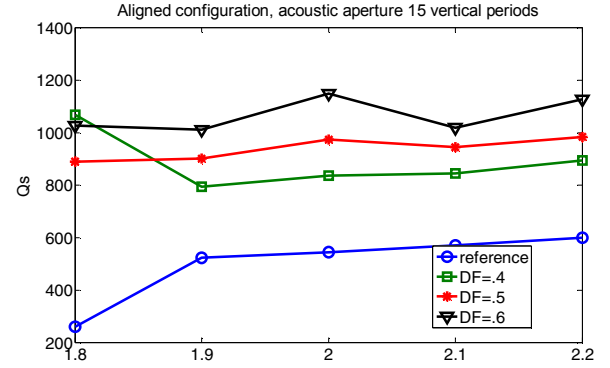
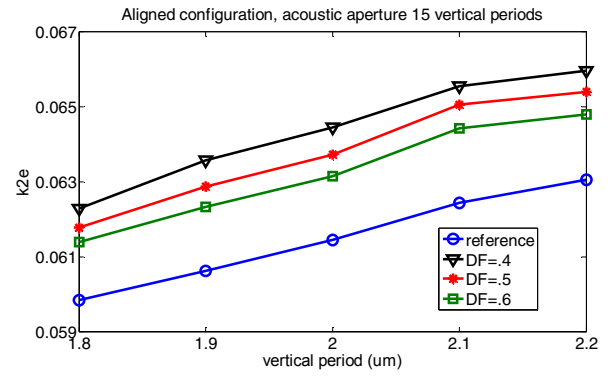


Figure 11. Experimental results for for the aligned dots devices in function of the vertical period in  $\mu\text{m}$ . The different curves correspond to the different vertical duty factors. The blue/circle symbols curve corresponds to the devices without tungsten dots. Top :coupling coefficient. Center: quality factor at resonance  $Q_s$ . Bottom: quality factor at antiresonance  $Q_p$  (bottom)

## REFERENCES

- [1] J. Koskela, J. V. Knuuttila, T. Makkonen, V. P. Plessky, M. M. Salomaa, "Acoustic Loss Mechanisms in Leaky SAW Resonators on Lithium Tantalate", IEEE Trans. On UFFC, vol. 48, no6, Nov 2001, pp 1517-1526
- [2] O. Holmgren, T. Makkonen, J. V. Knuuttila, V. P. Plessky, W. Steichen, "Laser-Interferometric Analysis of Rayleigh Wave Radiation from a LLSAW Resonator", 2007 IEEE Ultrasonics Symp. proc., pp 1905-1908
- [3] A. Khelif, B. Aoubiza, S. Mohammadi, A. Adibi, and V. Laude, "Complete band gaps in two-dimensional phononic crystal slabs," Phys. Rev. E 74, 046610 (2006)
- [4] P. Ventura, J. M. Hode, M. Solal, J. Desbois, J. Ribbe, "Numerical methods for SAW propagation characterization", 1998 IEEE Ultrasonics Symp. proc., pp 176-186